Comptes Rendus

Chimie

Bashdar I. Meena, Dóra Lakk-Bogáth, Soma Keszei and József Kaizer

Bleach catalysis in aqueous medium by iron(III)-isoindoline complexes and hydrogen peroxide

Full paper / *Article*

Bleach catalysis in aqueous medium by iron(III)-isoindoline complexes and hydrogen peroxide

Bashdar I. Meena[a], Dóra Lakk-Bogáth[a], Soma Keszei[a] and József Kaizer◉ [*, a]

[a] Research Group of Bioorganic and Biocoordination Chemistry, Universtiy of Pannonia, 8201 Veszprém, Hungary

E-mails: bashdarismael@gmail.com (B. I. Meena), bogidori@gmail.com
(D. Lakk-Bogáth), kornflakes09@gmail.com (S. Keszei), kaizer@almos.uni-pannon.hu
(J. Kaizer)

Abstract. Hydrogen peroxide and peroxymonocarbonate anion-based bleach reactions are important for many applications such as paper bleach, waste water treatment and laundry. Nonheme iron(III) complexes, $[Fe^{III}(L^{1-4})Cl_2]$ with the 1,3-bis(2′-Ar-imino)isoindolines ligands (HL^n, n =1–4, Ar = pyridyl, thiazolyl, benzimidazolyl and N-methylbenzimidazolyl, respectively) have been shown to catalyze the oxidative degradation of morin as a soluble model of a bleachable stain by H_2O_2 in buffered aqueous solution. In these experiments the bleaching activity of the catalysts was significantly influenced by the Lewis acidity and redox properties of the metal centers, and showed a linear correlation with the Fe^{III}/Fe^{II} redox potentials (in the range of 197–415 mV) controlled by the modification of the electron donor properties of the ligand introducing various aryl groups on the bisiminoisoindoline moiety. A similar trend but with low yields was observed for the disproportionation of H_2O_2 (catalase-like reaction) which is a major side reaction of catalytic bleach with transition metal complexes. The effect of bicarbonate ions might be explained by the reduction of Fe(III) ions and/or the formation of peroxymonocarbonate monoanion, which is a much stronger oxidant and could increase the formation of the catalytically active high-valent oxoiron species.

Keywords. Iron complexes, Isoindolines, Catalase activity, Bleach catalyst, Hydrogen peroxide.

Manuscript received 13th April 2021, revised 26th July 2021, accepted 24th August 2021.

1. Introduction

Oxidation reactions including low-cost and non-toxic transition metallic catalysts and green oxidants such as H_2O_2 have been extensively studied [1–4]. We have shown previously that iron, manganese, copper, cobalt and nickel 1,3-bis(2′-Ar-imino)isoindoline complexes can mediate many types of redox reactions depending on their oxidation state, redox potential and the choice of oxidant [5]. Depending on the substrate, these reactions have been used as functional models of superoxide dismutase [6–8], catalase [9–11], phenoxazinone synthase, catechol oxidase [12], catechol and flavonol dioxygenase enzymes [13,14]. Furthermore, their iron complexes can be used as catalysts for the oxidation of alcohols and sulfides [15,16]. The activity of the

* Corresponding author.

hydrogen peroxide-based bleach reactions can also be increased by the use of transition metal-based catalysts [17–19]. These include mainly manganese and iron complexes with salen, macrocyclic tetraamido and other polypyridyl-type ligands [20–30]. Recently, we synthesized a series of divalent manganese complexes $Mn^{II}(HL^{1-6})$ with the 1,3-bis(2′-Ar-imino)isoindolines and which are used as bleaching catalysts [31]. We have shown that the activity of the catalysts is significantly influenced by the Lewis acid and redox properties of the metal centers which can be controlled by varying the aryl substituent on the bis-iminoisoindoline moiety. The great variability of possible metal and ligand might result in a large variety of complexes with tunable catalytic properties. As a continuation of these studies, efforts have been made to evaluate the bleaching potential of our previously prepared $[Fe^{III}(L^{1-4})Cl_2]$ complexes by the use of morin as a model compound for bleaching stain, to understand how the parameters influence the activity and how the catalytic activity can be optimized compared to our manganese system (Scheme 1). These kinds of catalytic systems are increasingly important for many applications such as pulp and paper bleach and waste water treatment.

2. Experimental section

2.1. *Materials and methods*

The ligands 1,3-bis(2′-Ar-imino)isoindolines (HL^n, $n = 1$–4, Ar = pyridyl, thiazolyl, benzimidazolyl and *N*-methylbenzimidazolyl, respectively) and their complexes $[Fe^{III}(L^{1-4})Cl_2]$ (**1–4**) were prepared according to published procedures [5]. UV/Vis spectra were recorded with an Agilent 8453 diode-array spectrophotometer with quartz cells.

2.2. *Description of the catalytic bleaching*

Bleaching experiments were carried out as described previously for 1,3-bis(2′-Ar-imino)isoindoline manganese complexes to allow comparison of the two systems. Kinetics of morin bleach were monitored on an Agilent 8453 diode-array spectrophotometer using thermostated quartz cells equipped with a magnetic stirring unit. The initial absorbance of morin in buffer solution was measured, and its bleaching reaction was followed as the decrease in absorbance
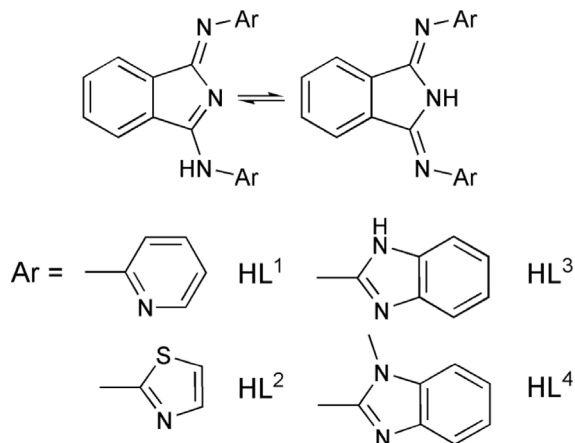
Scheme 1. Structure of the 1,3-bis(2′-Ar-imino)isoindoline ligands used for the synthesis of $[Fe^{III}(L^{1-4})Cl_2]$ (**1–4**) catalysts involved in this study.

at 410 nm. In a typical experiment, the cuvette ($l = 1$ cm) was filled with 3 mL buffer solution containing 0.62 μM catalyst, 160 μM morin, and the bleaching reaction initiated by adding 10 mM H_2O_2 into the reaction mixture (Tables 1 and 2). The pH was adjusted by 50 mM sodium carbonate–bicarbonate (CO_3^{2-}/HCO_3^-) buffer (pH 10) or 25 mM borax buffer (pH 8.5), respectively. First-order rate constants were calculated using Biochemical Analysis Software for Agilent ChemStation software.

2.3. *Description of the catalase-like activity*

Catalytic reactions were performed at 20 °C in a 30 mL thermostated reactor connected with a graduated burette filled with oil. To determine the time dependence of H_2O_2 decomposition, 0.211 mM (final concentration) of the complex dissolved in 1 mL DMF was added to 19 mL of a stirred sodium carbonate–bicarbonate (CO_3^{2-}/HCO_3^-) buffer solution (0.05 M $NaHCO_3$/0.1 M NaOH, pH 9.6) containing 0.447 M H_2O_2, and the evolved oxygen measured volumetrically at time intervals of 15 s. Initial rates were expressed as M·s^{-1} by taking the volume of the solution into account, and calculated from the maximum slope of the evolved dioxygen versus time (Tables 3 and 4).

Table 1. Summary of kinetic data for the catalytic oxidation of morin with [Fe^{III}(L^1)Cl$_2$] (**1**) in sodium carbonate–bicarbonate (CO$_3^{2-}$/HCO$_3^-$) buffer at pH 10 (and in borax buffer at pH 8.5) and 25 °C

[1] (10^{-7} M)	pH	[H$_2$O$_2$] (10^{-3} M)	[CO$_3^{2-}$/HCO$_3^-$] (10^{-3} M)	[Morin] (10^{-4} M)	k_{obs} (10^{-3} s^{-1})	k_{ox} (10^7 M^{-3}·s^{-1})
6.2	**8.5**	10	—	1.6	0.691	—
6.2	**10**	**10**	**50**	**1.6**	3.20	1.03 ± 0.03
16	10	10	50	1.6	8.10	1.01 ± 0.04
25	10	10	50	1.6	12.63	1.01 ± 0.06
6.2	10	**7.5**	50	1.6	2.43	1.04 ± 0.03
6.2	10	**5**	50	1.6	1.64	1.05 ± 0.02
6.2	10	**12**	50	1.6	3.90	1.04 ± 0.04
6.2	10	10	**100**	1.6	6.41	1.03 ± 0.02
6.2	10	10	**200**	1.6	12.53	1.01 ± 0.04
6.2	10	10	**300**	1.6	18.76	1.01 ± 0.04
6.2	10	10	50	**1.2**	3.27	1.05 ± 0.02
6.2	10	10	50	**0.8**	3.23	1.04 ± 0.03
6.2	10	10	50	**0.4**	3.26	1.05 ± 0.01

Table 2. Summary of kinetic data for the catalytic oxidation of morin with [Fe^{III}(L$^{1-4}$)Cl$_2$] (**1–4**) in sodium carbonate–bicarbonate (CO$_3^{2-}$/HCO$_3^-$) buffer at pH 10 and 25 °C

Cat.	k_{Fe} (10^3 s^{-1})	k_{ox} (10^7 M^{-3}·s^{-1})	E_{pa} (Fe^{III}/Fe^{II}) (mV)
1	5.011	1.03	415
2	2.253	0.45	302
3	1.615	0.32	229
4	1.255	0.25	197

([CO$_3^{2-}$/HCO$_3^-$] = 50 mM, [Fe] = 0.62 μM, [Morin] = 0.16 mM and [H$_2$O$_2$] = 10 mM).

3. Results and discussion

Porphyrin and phthalocyanine metal complexes are known for many transition metals, but iron and manganese metals are the most suitable choices for a wide range of oxidation reactions due to their variable oxidation states and readily tunable properties such as Lewis acidity and redox potentials [32–35]. The chemical modification of porphyrin led to the 1,3-bis(2′-Ar-imino)isoindolines, where the solubility, electronic structure and steric properties of the ligand as well as their complexes can be easily tuned, introducing various aryl groups on the bis-iminoisoindoline moiety [5]. This system resulted in several oxidation catalysts with high catalytic efficiencies and selectivities. Recently we reported a kinetic study of H$_2$O$_2$ and morin oxidation in aqueous solution by 1,3-bis(2′-Ar-imino)isoindoline manganese complexes, where both the catalase-like and the bleaching activity showed a linear correlation with the Mn^{III}/Mn^{II} redox potentials, and were remarkably influenced by the concentration of the bicarbonate ions [31]. We now report a kinetic study of the H$_2$O$_2$ and morin oxidation by 1,3-bis(2′-Ar-imino)isoindoline iron(III) complexes and compare the reactions of the manganese and iron catalysts.

3.1. *Catalytic oxidation of morin*

The bleaching activity of [Fe^{III}(L$^{1-4}$)Cl$_2$] (**1–4**) was investigated in the oxidation of morin dye as a model marker for wine stains, utilizing H$_2$O$_2$ as the cooxidant and bicarbonate as additive at 25 °C (Scheme 2). It is well known that H$_2$O$_2$ reacts with bicarbonate anion to generate the peroxymonocarbonate which is a promising oxidant for bleaching [36].

First we investigated the effect of the pH value of the aqueous solution and found that the best activity was observed at pH 10 for **1** (Figure 1). Lowering
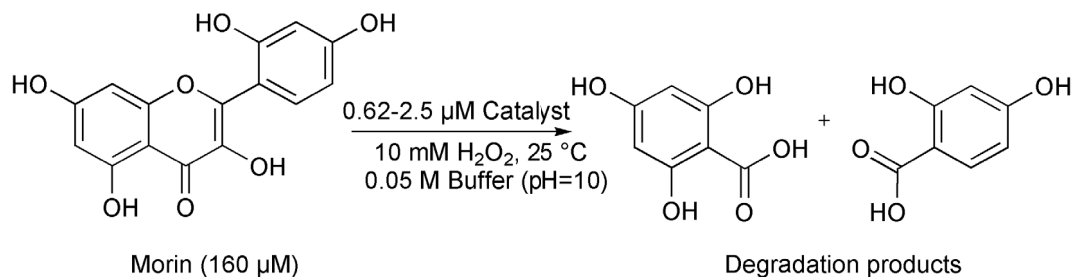
Scheme 2. Catalytic oxidation of morin by [Fe^{III}(L$^{1-4}$)Cl$_2$] (**1–4**) complexes.

Table 3. Comparison of the [Fe^{III}(L$^{1-4}$)Cl$_2$] (**1–4**) catalyzed disproportionation reaction of H$_2$O$_2$ in sodium carbonate–bicarbonate (CO$_3^{2-}$/HCO$_3^-$) buffer at pH 9.6 and 20 °C

Cat.	E_{pa}^o(Fe^{III}/Fe^{II}) (mV)	Yield (%)	TON[a]	TOF[b] (h^{-1})	V_0 (10^{-4} M·s^{-1})
1	415	21	451	9216	5.80
2	302	17	376	7164	3.95
3	229	11	239	5292	2.81
4	197	9	199	4428	2.30
FeCl$_3$	—	3.5	75	—	—

([Fe] = 0.211 mM and [H$_2$O$_2$] = 0.447 M).

[a] Turnover number = moles of converted substrate (H$_2$O$_2$)/moles of catalyst.

[b] Turnover frequency = TON/h.

Table 4. Bicarbonate dependence of the [Fe^{III}(L^1)Cl$_2$] (**1**) catalyzed disproportionation reaction of H$_2$O$_2$ in sodium carbonate–bicarbonate (CO$_3^{2-}$/HCO$_3^-$) buffer at pH 9.6 and 20 °C

Cat.	[CO$_3^{2-}$/HCO$_3^-$] (M)	Yield (%)	V_0 (10^{-4} M·s^{-1})
1	0.05	21	5.80
1	0.1	22	6.41
1	0.3	24	9.44
1	0.5	25	11.1
1	—	3.5	—

([Fe] = 0.211 mM and [H$_2$O$_2$] = 0.447 M).

Figure 1. Time-dependent UV–Vis spectra of a 0.16 mM solution of morin at pH 10 in the presence of 10 mM H$_2$O$_2$ and 0.62 μM [Fe^{III}(L^1)Cl$_2$] (**1**) at 25 °C. (Inset) Time course of the bleaching activity at pH 10 and pH 8.5.

the pH resulted in a significant drop in the observed reaction rates (k_{obs} = 3.2 × 10^{-3} s^{-1} at pH 10, and 0.691 × 10^{-3} s^{-1} at pH 8.5). This finding is consistent with the protonation state of the substrate (pKa values of morin are 3.5 and 8.1) and H$_2$O$_2$ (t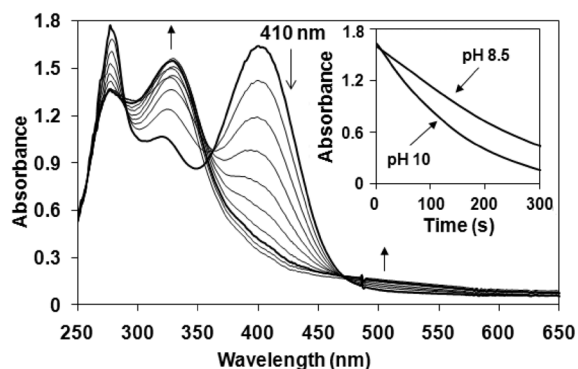he concentration of HOO$^-$ is high at pH 10), factors that determine the reactivity [19]. Under these conditions the bleaching of morin was completed within 5 min with approximately 45 catalytic cycles per minute
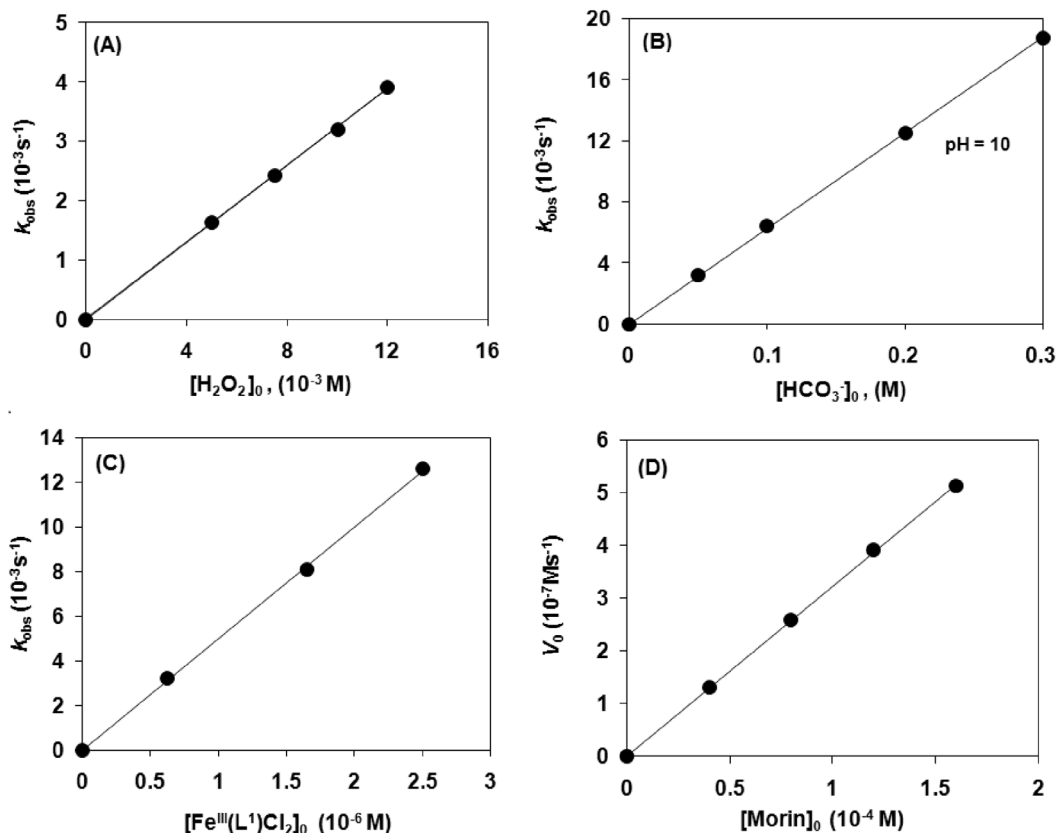
Figure 2. Catalytic oxidation of morin with $[Fe^{III}(L^1)Cl_2]$ (**1**) in sodium carbonate–bicarbonate (CO_3^{2-}/HCO_3^-) buffer at pH 10 and 25 °C. (A) Dependence of the first-order rate constant (k_{obs}) on the H_2O_2 concentration (Table 1). (B) Dependence of the first-order rate constant (k_{obs}) on the HCO_3^- concentration (Table 1). (C) Dependence of the first-order rate constant (k_{obs}) on the $[Fe^{III}(L^1)Cl_2]$ (**1**) concentration (Table 1). (D) Dependence of the initial reaction rate (V_o) on the morin concentration (Table 1).

(Figure 1). A similar, but slightly smaller value (~20) was observed for the analogous manganese(II) complex $[Mn^{II}(L^1)Cl_2]$ [31]. However, the bleaching activity of the 1,3-bis(2′-Py-imino)isoindoline iron(III) complex is at least 15–20 times smaller than that of manganese terpyridine (TOF ~ 800/min), and one order of magnitude smaller than that of iron phthalocyanine complexes [22].

To get more insight into the mechanism of this important reaction, detailed kinetic measurements were carried out. In order to determine the rate dependence on the various reactants, oxidation runs were performed with only the initial concentration of one reactant being varied and the other three initial concentrations remaining the same (pseudo-

first-order conditions). The concentrations related to the investigation of catalyst dose variations were as follows; [**1**]:[**H_2O_2**]:[HCO_3^-]:[Morin] = (**6.2 – 25**) × **10^{-4}**:10:50:0.16 mM. In the case of oxidant variation; [**1**]:[**H_2O_2**]:[HCO_3^-]:[Morin] = 6.2 × 10^{-4}:(**5–12**):50:0.16 mM. In the case of bicarbonate variation; [**1**]:[H_2O_2]:[**HCO_3^-**]:[Morin] = 6.2 × 10^{-4}:10:(**50–300**):0.16 mM). Finally, in the case of substrate variation; [**1**]:[H_2O_2]:[HCO_3^-]:[**Morin**] = 6.2 × 10^{-4}:50:50:(**0.04–0.16**) mM. The results from the investigation are summarized in Figures 2A–D.

Based on these results, the rate of morin decomposition can be described by the following equation, $-d[\text{morin}]/dt = V = k_{ox}[\mathbf{1-4}][H_2O_2][HCO_3^-][\text{Morin}]$, where $k_{ox} = 1.03 \times 10^7$ M^{-3}·s^{-1} for **1** and 0.25 ×

10^7 $M^{-3} \cdot s^{-1}$ for **4**. The bleaching activity of the pyridyl containing complex was at least four times higher than that of $[Fe^{III}(L^4)Cl_2]$ (**4**) with benzimidazolyl side chains. A similar trend was observed for the analogous $[Mn^{II}(HL^{1-4})Cl_2]$ system, where the k_{ox} value of $[Mn^{II}(HL^1)Cl_2]$ with pyridyl arms ($k_{ox} = 0.53 \times 10^7$ $M^{-3} \cdot s^{-1}$) was twice as small as that of **1** under the same conditions. We can conclude that the iron complex shows a significantly higher activity than the corresponding manganese complex. In summary, the reaction shows first-order dependence with all reactants; H_2O_2 (Figure 2A), HCO_3^- (Figure 2B), $[Fe^{III}(L^1)Cl_2]$ (Figure 2C) and morin (Figure 2D).

Similarly to our system, the non-innocent role of the phosphate and sodium carbonate–bicarbonate (CO_3^{2-}/HCO_3^-) buffers has been established in the H_2O_2 oxidative decomposition of various aromatic pollutants, catalyzed by iron(III) tetrasulfophthalocyanine [37] and iron(III) TAML complexes [38]. In the latter case, it was clearly revealed that picric acid was not oxidized in their absence. The role of buffer components has been clarified by kinetic measurements, which was of first order in the concentration of the catalyst, and showed ascending hyperbolic dependencies in the concentrations of H_2O_2, substrate and phosphate/carbonate, suggesting pre-equilibrium processes before the rate-determining step. Our results are in line with the above. The key step is the formation of the high-valent oxoiron species, which can be explained by two alternative mechanisms (Scheme 3).

The increase in activity in the presence of HCO_3^- might in part be caused by a direct interaction of the deprotonated HOO^- anion with the coordinated (Route 1a in Scheme 3) or noncoordinated (Route 1b in Scheme 3) bicarbonate anion in a nucleophilic step resulting in their partial conversion to peroxymonocarbonate monoanion (HCO_4^-). This species is a much stronger oxidant than H_2O_2 and could increase the formation rate of the catalytically active high-valent oxoiron species, which is responsible for the morin (H_2O_2) oxidation (Scheme 3).

The beneficial effect of HCO_3^- on iron reduction has also been postulated in the presence of various chelating ligands [39]. Morin as a chelating ligand is a good candidate for the complexation with Fe(III). This equilibrium step above can be supported by the first-order dependence on the morin concentration
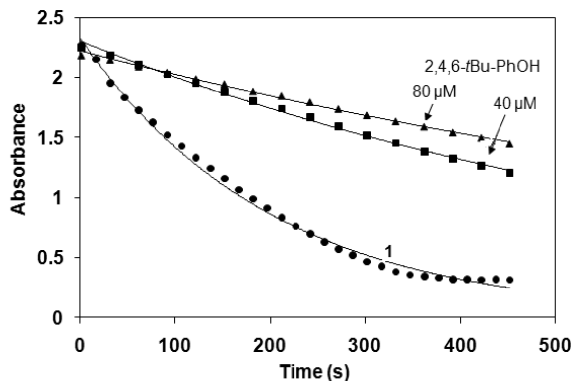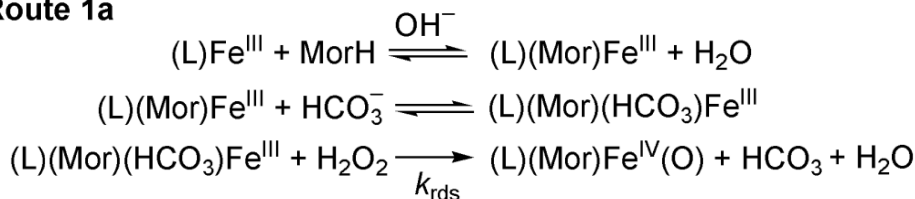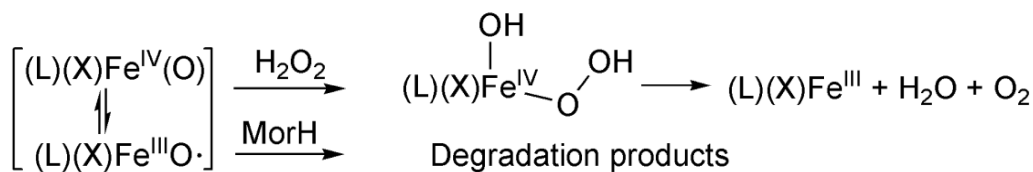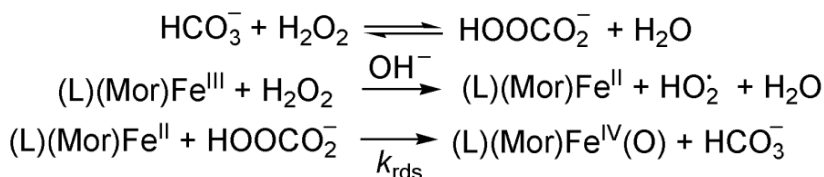

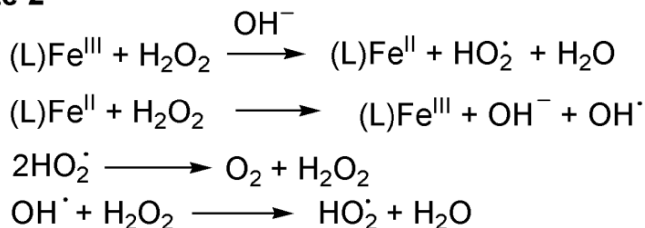**Figure 3.** Time course of the bleaching activity in the absence and in the presence of 2,4,6-*t*Bu-PhOH at pH 10 and 25 °C ([**1**] = 0.62 μM and [H_2O_2] = 10 mM).

and the appearance of a new absorption band in the spectrum (~450–500 nm), which can be assigned to the formation of stable five-membered chelate ring with the iron(III) ion [40–42]. It can also been seen that the reaction was significantly inhibited by the use of sterically hindered 2,4,6-tri-*tert*-butyl phenol (2,4,6-*t*Bu-PhOH) as •OH scavenger (Figure 3). In this manner, the formation of hydroxyl radicals and their non-selective reactions cannot be excluded, but for the bleaching applications a distinction between •OH and a high-valent oxoiron species may not be necessary. In summary, the mechanism of the bleaching reaction might be explained by the parallel selective metal-based, and non-selective radical processes (Scheme 4), where the first step is the hydrogen atom transfer (HAT), resulting in the formation of morin radical. This radical can then easily react with dioxygen and/or hydroperoxyl radical forming 1,4-endoperoxide, which decomposes by loss of CO to substituted O-benzoylsalicylic acid and their hydrolyzed products [43], similarly to a quercetinase enzyme reaction [42]. The base-catalyzed air oxidation of morin is negligible under our conditions [40,41].

The modification of the ligand in the model catalysts (pyridyl (**1**), thiazolyl (**2**), benzimidazolyl (**3**) and N-methylbenzimidazolyl (**4**) show a decreasing reaction rate in the listed order (Figure 4A). The cyclic voltammograms of the catalysts **1**–**4** exhibited a decreasing oxidation potential in DMF, **1** = 415, **2** = 302, **3** = 222 and **4** = 197 mV (100 mV·s^{-1} scan rate, Fc/Fc$^+$

Route 1a

$$(L)Fe^{III} + MorH \underset{}{\overset{OH^-}{\rightleftharpoons}} (L)(Mor)Fe^{III} + H_2O$$

$$(L)(Mor)Fe^{III} + HCO_3^- \rightleftharpoons (L)(Mor)(HCO_3)Fe^{III}$$

$$(L)(Mor)(HCO_3)Fe^{III} + H_2O_2 \xrightarrow{k_{rds}} (L)(Mor)Fe^{IV}(O) + HCO_3 + H_2O$$

Route 1b

$$HCO_3^- + H_2O_2 \rightleftharpoons HOOCO_2^- + H_2O$$

$$(L)(Mor)Fe^{III} + H_2O_2 \xrightarrow{OH^-} (L)(Mor)Fe^{II} + HO_2^{\cdot} + H_2O$$

$$(L)(Mor)Fe^{II} + HOOCO_2^- \xrightarrow{k_{rds}} (L)(Mor)Fe^{IV}(O) + HCO_3^-$$

$$\begin{bmatrix} (L)(X)Fe^{IV}(O) \\ \updownarrow \\ (L)(X)Fe^{III}O\cdot \end{bmatrix} \xrightarrow[\text{MorH}]{H_2O_2} \quad (L)(X)Fe^{IV}\underset{O}{\overset{OH}{\diagdown}}\diagup^{OH} \longrightarrow (L)(X)Fe^{III} + H_2O + O_2$$

$$\text{Degradation products}$$

$$X = Solv \text{ or } MorH$$

Route 2

$$(L)Fe^{III} + H_2O_2 \xrightarrow{OH^-} (L)Fe^{II} + HO_2^{\cdot} + H_2O$$

$$(L)Fe^{II} + H_2O_2 \longrightarrow (L)Fe^{III} + OH^- + OH^{\cdot}$$

$$2HO_2^{\cdot} \longrightarrow O_2 + H_2O_2$$

$$OH^{\cdot} + H_2O_2 \longrightarrow HO_2^{\cdot} + H_2O$$

Scheme 3. Proposed mechanism of bleaching reaction and H_2O_2 disproportionation.

internal standard, 0.1 M) (Table 3) [13,44]. The decrease in the redox potential stabilizes the Fe(III) state, while the increase in it makes the Fe(III) center more easily reducible, stabilizing the iron(II) form. This is in agreement with the assumption that a faster reaction rate is observed with higher oxidation potential of the catalyst (**1**) (Figure 4B). Figure 4B shows that complex **1** with pyridine arms is the best oxidant and has the highest k_{Fe} among these complexes.

3.2. *Catalytic oxidation of H_2O_2*

Our model experiments with morin revealed that the complexes are relatively stable under aqueous alkaline conditions in the presence of hydrogen peroxide and bicarbonate ions, and the optimal pH for bleaching activity is around 10, where the reactivity values are slightly higher than those of analogous manganese complexes. To get high bleach (or oxidation) performance, one of the most important criteria of the catalysts, is that it must possess a low activity to catalyze the non-productive decomposition of H_2O_2. This process is the major side reaction of the transition metal catalysts. To test the catalase-like activity of the 1,3-bis(2′-Ar-imino)isoindoline-iron(III) complexes the reactions were performed in alkaline aqueous solution at pH 9.6 (sodium carbonate–bicarbonate (CO_3^{2-}/HCO_3^-) buffer) and 20 °C (Figure 5). Figure 5A shows the time dependence of the
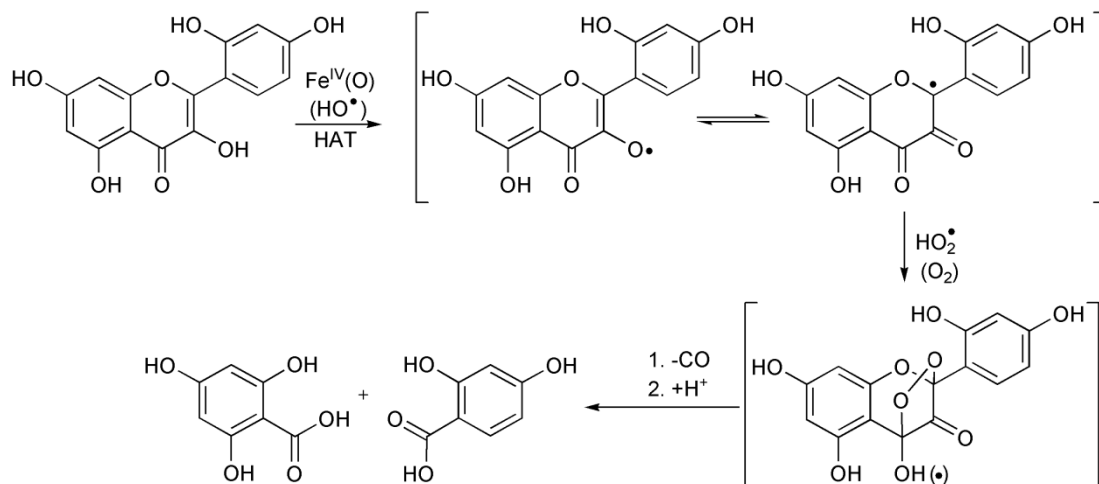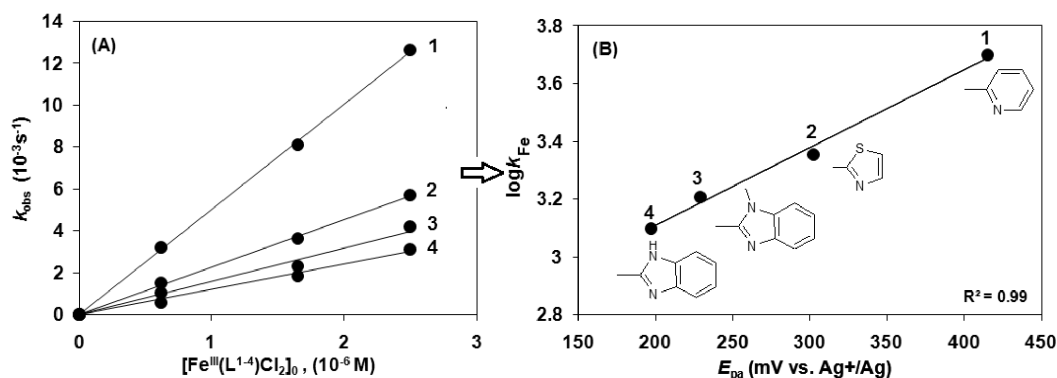
Scheme 4. Proposed mechanism of the morin oxidation.

Figure 4. Catalytic oxidation of morin with $[Fe^{III}(L^{1-4})Cl_2]$ (**1–4**) in sodium carbonate–bicarbonate (CO_3^{2-}/HCO_3^-) buffer at pH 10 and 25 °C (Table 2). (A) Dependence of the first-order rate constant (k_{obs}) on the $[Fe^{III}(L^{1-4})Cl_2]$ (**1–4**) concentration (Table 2). (B) Dependence of the rate constant (k_{Fe}) on the oxidation potential (E_{pa}) of the $[Fe^{III}(L^{1-4})Cl_2]$ (**1–4**) complexes in sodium carbonate–bicarbonate (CO_3^{2-}/HCO_3^-) buffer (pH 10).

disproportionation of H_2O_2, measuring the evolved dioxygen. It took less than 3 min to have about 21% yield (TON = 451 based on H_2O_2) for complex **1** and it decreases in the order **2** (17%) > **3** (11%) > **4** (9%). A much lower yield was obtained for $FeCl_3$ (~2%) (Table 3). It is worth noting that complex $[Fe^{III}(L^1)Cl_2]$ (**1**) is a less efficient catalyst (catalase mimic) when compared to the previously published manganese analogous $[Mn^{II}(HL^1)Cl_2]$ (Yield = 33%, TON = 692 for H_2O_2 decomposition). It is worth noting that most of the used catalysts bleach

well with the peroxide level typically present in the detergents.

Based on kinetic studies, the reaction rate is directly proportional to the concentration of H_2O_2 and shows *Michaelis–Menten*-type saturation kinetics on $[HCO_3^-]_0$ with $V_{max} = 1.29(6) \times 10^{-3}$ M·s^{-1}, $K_M = 96$ mM, $k_c = 6.1$ s^{-1} at 20 °C, establishing a pre-equilibrium process (Figure 6A). Similarly to the bleaching process including both the 1,3-bis(2′-Ar-imino)isoindoline-iron(III) and manganese(II) systems, the higher the redox potentials of the
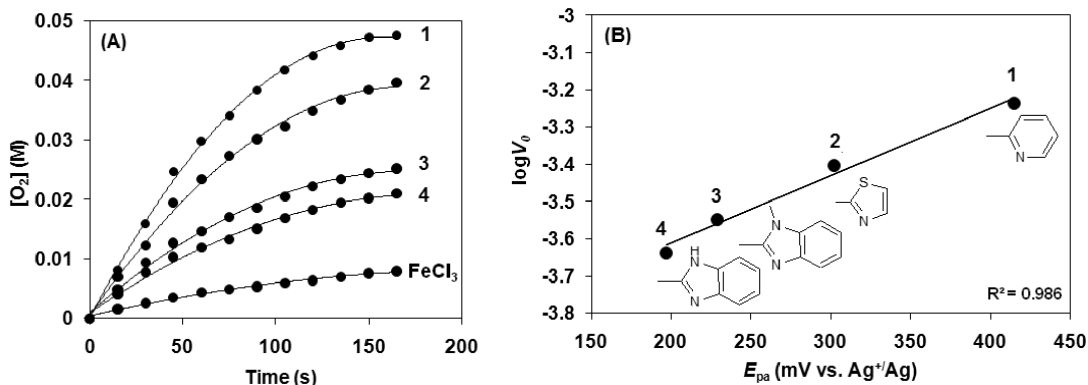
Figure 5. Kinetic analysis for the hydrogen peroxide disproportionation catalyzed by $[\text{Fe}^{III}(\text{L}^{1-4})\text{Cl}_2]$ (**1–4**) complexes in sodium carbonate–bicarbonate ($\text{CO}_3^{2-}/\text{HCO}_3^-$) buffer at pH 9.6 and 20 °C (Table 3). (A) Time traces for reaction of $[\text{Fe}^{III}(\text{L}^{1-4})\text{Cl}_2]$ (**1–4**) with H_2O_2 in the presence of bicarbonate ions. (B) Dependence of the reaction rate on the oxidation potential (E_{pa}) of the $[\text{Fe}^{III}(\text{L}^{1-4})\text{Cl}_2]$ (**1–4**) (Table 3).
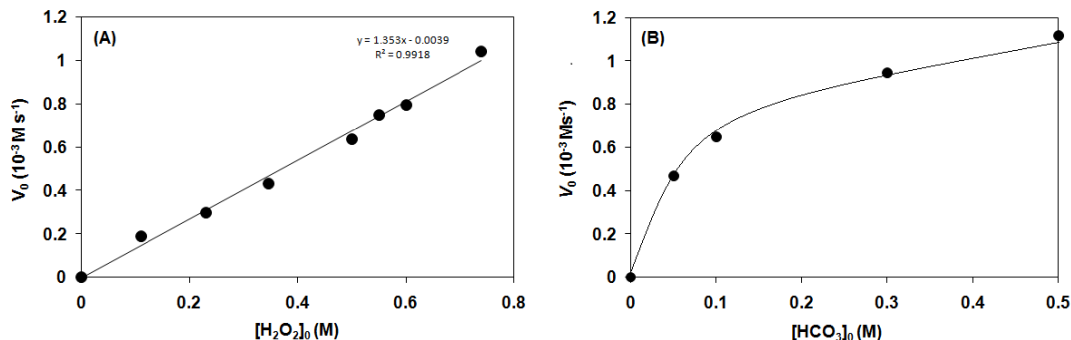

Figure 6. Kinetic analysis for the hydrogen peroxide disproportionation catalyzed by $[\text{Fe}^{III}(\text{L}^1)\text{Cl}_2]$ (**1–4**) complexes in sodium carbonate–bicarbonate ($\text{CO}_3^{2-}/\text{HCO}_3^-$) buffer at pH 9.6 and 20 °C (Table 3). (A) Dependence of the initial reaction rate (V_o) on the H_2O_2 concentration. (B) Dependence of the initial reaction rate (V_o) on the HCO_3^- concentration. Conditions: $[\mathbf{1}]_0 = 2.11 \times 10^{-4}$ M.

$\text{Fe}^{III}/\text{Fe}^{II}$ redox couple (E_{pa}), the higher the rate of the H_2O_2 disproportionation ($\log V_0$) which means that the catalyst which is easier to reduce reacts faster, the electron-deficient (Lewis acid) catalyst (**1**) is much more active than the electron-rich derivatives (**3**, **4**) (Figure 6B).

4. Conclusion

We have found that our simple 1,3-bis(2′-Ar-imino)isoindoline iron(III) complexes effectively oxidize the morin in aqueous solution under mild conditions in the presence of bicarbonate ions. We have also found that increasing the Lewis acidity and

oxidation potentials (E_{pa}) of the catalyst by introducing pyridine arms on the bis-iminoisoindoline moiety significantly improves the bleach performance in model experiments under European washing conditions at 25 °C. The optimal pH for bleaching activity is about 10, and our catalysts possess a relatively low activity for the disproportionation of hydrogen peroxide. Based on detailed kinetic measurements the bleaching rates depend on the initial concentrations of each reactant. Since the sterically hindered phenols inhibited the reaction, the radical chain mechanism cannot be excluded. The beneficial effect of bicarbonate ions might be explained by the reduction of iron(III) to iron(II) complexes, and the forma-

tion of the peroxymonocarbonate monoanion which is a much stronger oxidant than H_2O_2, and could easily form a catalytically active high-valent oxoiron species with the iron(II) form. Similar results, trends, and mechanisms were observed for the analogous 1,3-bis(2′-Ar-imino)isoindoline manganese(II) complexes, but with lower bleaching and slightly higher catalase-like activities.

Conflicts of interest

The authors declare that they have no known competing financial interests or personal relationships that could have appeared to influence the work reported in this paper.

Acknowledgments

References

[1] B. Sorokin, *Chem. Rev.*, 2013, **113**, 8152-8191.
[2] S. Tanase, J. Reedijk, R. Hage, G. Rothenberg, *Top. Catal.*, 2010, **53**, 1039-1044.
[3] B. Shul'pin, C. C. Golfeto, G. Süss-Fink, L. S. Shul'pina, D. Mandelli, *Tetrahedron Lett.*, 2005, **46**, 4563-4567.
[4] N. Bilyachenko, M. M. Levitsky, A. I. Yalymov, A. A. Korlyukov, V. N. Khrustalev, A. V. Vologzhanina, L. S. Shul'pina, N. S. Ikonnikov, A. E. Trigub, P. V. Dorovatovsky, X. Bantreil, F. Lamaty, J. Long, J. Larionova, I. E. Golub, E. S. Shubina, G. B. Shul'pin, *Angew. Chem. Int. Ed.*, 2016, **55**, 15360-15363 (English version).
[5] R. Csonka, G. Speier, J. Kaizer, *RSC Adv.*, 2015, **5**, 18401-18419.
[6] B. Kripli, G. Baráth, É. Balogh-Hergovich, M. Giorgi, A. J. Simaan, L. Párkányi, J. S. Pap, J. Kaizer, G. Speier, *Inorg. Chem. Commun.*, 2011, **14**, 205-209.
[7] J. S. Pap, B. Kripli, T. Váradi, M. Giorgi, J. Kaizer, G. Speier, *J. Inorg. Biochem.*, 2011, **105**, 911-918.
[8] J. S. Pap, B. Kripli, V. Bányai, M. Giorgi, L. Korecz, T. Gajda, D. Árus, J. Kaizer, G. Speier, *Inorg. Chim. Acta*, 2011, **376**, 158-169.
[9] J. Kaizer, G. Baráth, G. Speier, M. Réglier, M. Giorgi, *Inorg. Chem. Commun.*, 2007, **10**, 292-294.
[10] J. Kaizer, B. Kripli, G. Speier, L. Párkányi, *Polyhedron*, 2009, **28**, 933-936.
[11] J. Kaizer, T. Csay, P. Kővári, G. Speier, L. Párksányi, *J. Mol. Catal. A Chem.*, 2008, **280**, 203-209.
[12] J. Kaizer, G. Baráth, R. Csonka, G. Speier, L. Korecz, A. Rockenbauer, L. Párkányi, *J. Inorg. Biochem.*, 2008, **102**, 773-780.
[13] T. Váradi, J. S. Pap, M. Giorgi, L. Párkányi, T. Csay, G. Speier, *Inorg. Chem.*, 2013, **52**, 1559-1569.
[14] É. Balogh-Hergovich, J. Kaizer, G. Speier, G. Huttner, A. Jacobi, *Inorg. Chem.*, 2000, **39**, 4224-4229.
[15] J. S. Pap, M. A. Cranswick, É. Balogh-Hergovich, G. Baráth, M. Giorgi, G. T. Rohde, J. Kaizer, G. Speier, L. Que Jr, *Eur. J. Inorg. Chem.*, 2013, 3858-3866.
[16] B. Kripli, M. Szávuly, F. V. Csendes, J. Kaizer, *Dalton Trans.*, 2020, **49**, 1742-1746.
[17] P. Sen, E. Yildirim, S. Z. Yildiz, *Synth. Met.*, 2016, **215**, 41-49.
[18] P. Sen, S. Z. Yildiz, *Inorg. Chim. Acta*, 2017, **462**, 30-39.
[19] T. Wieprecht, M. Hazenkamp, H. Rohwer, G. Schlingloff, J. Xia, *C. R. Chim.*, 2007, **10**, 326-340.
[20] E. Ember, H. A. Gazzaz, S. Rothbart, R. Puchta, R. van Eldik, *Appl. Catal. B Environ.*, 2010, **95**, 179-191.
[21] R. Hage, A. Lienke, *J. Mol. Catal. A Chem.*, 2006, **251**, 150-158.
[22] A. B. Sorokin, E. V. Kudrik, *Catal. Today*, 2011, **159**, 37-46.
[23] T. Wieprecht, J. Xia, U. Heinz, J. Dannacher, G. Schlingloff, *J. Mol. Catal. A Chem.*, 2003, **203**, 113-128.
[24] R. Hage, A. Lienke, *Angew. Chem. Int. Ed.*, 2006, **45**, 206-222.
[25] J. J. Dannacher, *J. Mol. Catal. A Chem.*, 2006, **251**, 159-176.
[26] G. Reinhardt, *J. Mol. Catal. A Chem.*, 2006, **251**, 177-184.
[27] T. J. Collins, *Acc. Chem. Res.*, 2002, **35**, 782-790.
[28] T. J. Collins, C. P. Horwitz, A. D. Ryabov, L. D. Vuocolo, S. S. Gupta, A. Ghosh, N. L. Fattaleh, Y. Hangun, B. Steinhoff, C. A. Noser, E. Beach, D. Prasihn Jr, T. Stuthridge, K. G. Wintage, J. Hall, L. J. Wright, I. Suckling, R. W. Allison, *ACS Symp. Ser.*, 2002, **823**, 47-60.
[29] C. P. Horwitz, T. J. Collins, J. Spatz, H. J. Smith, L. J. Wright, T. R. Stuthridge, K. G. Wingate, K. McGrouther, *ACS Symp. Ser.*, 2006, **921**, 156-169.
[30] K. G. Wingate, T. R. Stuthridge, L. J. Wright, C. P. Horwitz, T. J. Collins, *Water Sci. Technol.*, 2004, **49**, 255-260.
[31] B. I. Meena, J. Kaizer, *Catalysts*, 2020, **10**, 404-418.
[32] B. Meunier, A. Sorokin, *Acc. Chem. Res.*, 1997, **30**, 470-476.
[33] S. Mangematin, A. B. Sorokin, *J. Porphyri. Phthalocyanines*, 2001, **5**, 674-680.
[34] A. Sorokin, J.-L. Séris, B. Meunier, *Science*, 1995, **268**, 1163-1166.
[35] A. Sorokin, B. Meunier, *Chem. Eur. J.*, 1996, **2**, 1308-1317.
[36] F. K. Attiogbe, R. C. Francis, *Can. J. Chem.*, 2011, **89**, 1289-1296.
[37] M. Sanchez, A. Hadasch, R. T. Fell, B. Meunier, *J. Catal.*, 2001, **202**, 177-186.
[38] S. Kundu, L. Q. Shen, Y. Somasundar, M. Annavajhala, A. D. Ryabov, T. J. Collins, *Inorg. Chem.*, 2020, **59**, 13223-13232.
[39] F. Müller, J. Rapp, A. L. Hacker, A. Feith, R. Takors, B. Blombach, *mBio*, 2020, **11**, article no. e00085-20.
[40] J. S. Pap, J. Kaizer, G. Speier, *Coord. Chem. Rev.*, 2010, **254**, 781-793.
[41] J. Kaizer, É. Balogh-Hergovich, M. Czaun, T. Csay, G. Speier, *Coord. Chem. Rev.*, 2006, **250**, 2222-2233.
[42] A. Matuz, M. Giorgi, G. Speier, J. Kaizer, *Polyhedron*, 2013, **63**, 41-49.
[43] J. Kaizer, G. Speier, *J. Mol. Catal. A Chem.*, 2001, **171**, 33-36.
[44] M. Szávuly, R. Csonka, G. Speier, R. Barabás, M. Giorgi, J. Kaizer, *J. Mol. Catal. A Chem.*, 2014, **392**, 120-126.